

On the formation of an oxycarbonate intermediate phase in the synthesis of BaTiO₃ from (Ba,Ti)-polymeric organic precursors

Pedro Durán^{a,*}, Dionisio Gutierrez^a, Jesús Tartaj^a, Miguel A. Bañares^b, Carlos Moure^a

^a*Instituto de Cerámica y Vidrio (CSIC), Electroceramics Department, 28500-Arganda del Rey, Madrid, Spain*

^b*Instituto de Catálisis y Petroleoquímica (CSIC), Campus UAM, Cantoblanco, 28049, Madrid, Spain*

Received 2 April 2001; received in revised form 19 June 2001; accepted 9 July 2001

Abstract

The study of BaTiO₃ crystallization from X-ray amorphous (Ba,Ti) polymeric organic powders has been carried out on a (Ba,Ti)-citrate polymeric resin heat-treated in air at 250 °C. From thermal analysis, X-ray diffraction, infrared and Raman spectroscopies, and ¹³C NMR spectroscopy, it has been concluded that an intermediate oxycarbonate phase was formed prior to the formation of BaTiO₃ above 550 °C. Although not well crystallized, thermoanalytical measurements, the unique XRD pattern, and new IR, Raman, and ¹³C NMR structural features revealed that such a metastable intermediate oxycarbonate phase has a stoichiometry close to Ba₂Ti₂O₅CO₃, which is characterized by having CO₃²⁻ groups different to those of pure BaCO₃ located, probably, in an open interlayer BaTiO₃ metastable structure. A tentative structure for the oxycarbonate phase is proposed. From the XRD crystal size measurements and Raman spectra, it was suggested that the thermal decomposition of the (Ba, Ti) citrate polymeric organic precursor above 550 °C led to the formation of a mixture of tetragonal and hexagonal BaTiO₃ polymorphs rather than cubic. Despite the specific surface of the synthesized BaTiO₃ powders up to 700 °C, higher than 40 m²/g and an equivalent particle size smaller than 25 nm, Raman spectra indicated asymmetry inside the TiO₆ octahedra of the BaTiO₃ structure. © 2002 Published by Elsevier Science Ltd.

Keywords: BaTiO₃; Ba₂Ti₂O₅CO₃; Powders-chemical preparation; Precursors-organic; Reaction sequence

1. Introduction

Although a number of investigations have contributed to a better knowledge of the reactions involved in the thermal decomposition method of synthesis to BaTiO₃,^{1–6} there have been four major efforts over the last 25 years to establish as unambiguously as possible the reaction mechanism(s) taking place during the thermal decomposition of the (Ba,Ti)-polymeric organic precursors for the BaTiO₃ formation.^{7–10}

Gopalakrishnamurthy et al.⁷ were the first reporting the existence of an oxycarbonate like intermediate phase (Ba₂Ti₂O₅CO₃) as the key for the formation of BaTiO₃ during the thermolysis of barium titanyl oxalate in air. Hennings and Mayr⁸ studied the thermal decomposition of (Ba,Ti)-citrate salts and assuming a complete molecular-level mixing of barium and titanium cations,

concluded that prior to the formation of BaTiO₃ an intermediate with the overall composition BaCO₃TiO₂ was formed. In both cases the conclusions were based on the obtained experimental results using the classical techniques such as XRD, TG/DTA, and IR. Albeit with some discrepancy on the types of intermediate phases involved, it was accepted that the formation of BaTiO₃ from the thermal decomposition of organic precursors involves the following three main steps as the calcining temperature was increased: (i) dehydration reaction, (ii) decomposition/oxidation reactions of the organic species to form intermediate phases such as BaCO₃, TiO₂, BaCO₃ TiO₂ and Ba₂Ti₂O₅ CO₃, and (iii) reaction between the formed intermediate phases or the decomposition of the metastable Ba₂Ti₂O₅CO₃ phase leading to the formation of BaTiO₃ as the final reaction product.

Kumar et al.⁹ on the basis of XRD, TG/DTA, and Raman spectrometry data, found that an oxycarbonate intermediate phase, and not a mixture of BaCO₃ and TiO₂, as proposed by Henning and Mayr,⁸ forms in the

* Corresponding author. Tel.: +34-91-871-1800; fax: +34-91-870-0550.

E-mail address: pduran@icv.csic.es (P. Durán).

thermal decomposition of (Ba,Ti)-citrate based organic precursors previously heat-treated at 375 °C for 10 h. The stoichiometry of such an intermediate phase was considered to be close to $\text{Ba}_2\text{Ti}_2\text{O}_5\text{CO}_3$, and the BaTiO_3 was formed from the endothermic decomposition of the intermediate phase in the temperature interval of 635–700 °C.

Recently, Durán et al.¹⁰ reported, although not conclusively, that depending on the heating rate the BaTiO_3 formation could take place via a predominant solid-state reaction, between nanosized BaCO_3 particles and amorphous $\text{TiO}_2(\text{TiO}_{2-x})$ when crystallized by low heating rate (< 1.5 °C/min), although a relatively small amount of a quasi-amorphous oxycarbonate intermediate phase was also present. BaTiO_3 crystallization by rapid heating-rate (≥ 5 °C/min) took place through a quasi-amorphous oxycarbonate phase formation, as the main rate-controlling factor for the crystallization process. The formation of an oxygen-deficient hexagonal BaTiO_3 coexisting with tetragonal BaTiO_3 polymorph up to 700 °C also was suggested.

In all the above mentioned contributions, a common fact, the formation of an oxycarbonate phase alone or accompanied by other by-products, was reported as the controlling-rate factor for the BaTiO_3 formation. More recently, Gablenz et al.¹¹ have shown an additional evidence for the existence of such an oxycarbonate intermediate phase based on the electron energy loss spectroscopy (EELS) measurements, and quantum-mechanical calculations using density functional theory (DFT). However its formation, nature, stability, and the role played during the synthesis of BaTiO_3 , have not unambiguously clarified and in some cases questioned.^{12,13}

Based on our previous studies,¹⁰ we believe that the mechanism of the BaTiO_3 synthesis can change not only with the heating rate regime but also with the previous thermal history of the polymeric precursors. In the present paper the thermal behavior of the polymeric precursors previously heat-treated at 250 °C is studied, and an attempt to synthesize the oxycarbonate intermediate phase from the (Ba,Ti)-citrate polymerized amorphous precursors, is undertaken. Its characterization using TG/DTA, XRD, IR, and ^{13}C NMR techniques will be carried out. Its stability and thermal evolution leading to the BaTiO_3 formation will also be studied using XRD, IR and room temperature Raman spectroscopies.

2. Experimental procedure

2.1. Preparation of the powder precursors

The details of the powder preparation method have been reported elsewhere¹⁰. Briefly, a slightly acidified ethylene glycol (EG) solution of titanium tetrabutoxide

was mixed with an aqueous citric acid (CA) solution by stirring and heated at 60 °C for 2 h. The clear obtained solution was then mixed with an aqueous barium nitrate solution $\text{Ba}(\text{NO}_3)_2$ (99.99%, Aldrich), such that the moles of barium equaled the moles of titanium. A molar ratio of $\text{Ba/Ti/CA/EG} = 0.1/0.1/1/4$ was used. This liquid mix solution was heated up to 80 °C for 2 h. A transparent organic solution was obtained indicating that the mixing of barium and titanium cations was on the molecular level. In order to promote the esterification reaction the above clear organic solution was heated up to 130 °C for 2 h. A change to pale yellow in the color of the solution took place at this step. Then the solution was concentrated by heating up to 180 °C for 3 h. The solution became more viscous and changed its color to brown. No visible precipitation was observed along such heating process. Finally the viscous solution was heated up to 250 °C for several hours, and a solidified dark brown spongy resin, hereinafter referred to as the “polyester resin” or PR powder, was obtained. The “polyester resin” was converted into a powder by grinding with a teflon bar, and all further thermal analyses were performed on such a precursor powder.

2.2. Powder characterization

The thermal analyses were carried out with a thermoanalyser (STA 409, Netzsch-Geratebau, Selb-Bayern, Germany) which record DTA and TG simultaneously. 150 mg samples were placed in platinum crucibles, using calcined alumina as a reference material. The heating rate was 10 °C/min and the thermal analyses were carried out in flowing air. The resultant phases in the “polyester resin” heat-treated in the temperature range of 400–750 °C, were identified by X-ray diffraction (XRD), $\text{CuK}\alpha$, 50 kV-30 mA (Siemens D-5000, Erlangen, Germany). The scan rate was $2^\circ 2\theta/\text{min}$ for the phase identification in the 2θ range $2-75^\circ$ and step scanning (step size 0.002 counting time $10^\circ/\text{step}$) was used for the determination of the lattice parameters, where standard silicon powder was used for the angle calibration. Crystallite sizes of calcined powders were determined by X-ray line broadening using the Scherrer equation.¹⁴ The specific surface area of the calcined powders was measured with nitrogen by single-point BET (Quantachrome MS-16 model, Syosset, NY). IR spectra were recorded with a FT-IR spectrometer (Perkin-Elmer 1760 X, Beaconsfield, UK) in the range of $400-4000\text{ cm}^{-1}$ on as pressed disks using KBr as binding material. IR spectra were used to characterize the coordination made in the heat-treated (Ba,Ti)-polymeric precursors.

The molecular structure and cation coordination in the calcined powder precursors were studied using Raman spectroscopy. Raman spectra were registered at

room temperature with a single monochromatic Renishaw system 1000 equipped with a cooled CCD detector (200 K) and a holographic Notch filter. The elastic scattering is filtered by the holographic Notch filter, and the Raman signal remains higher than with the triple monochromatic spectrometers. The samples were excited with the 514-nm Ar line in in-situ treatments. The resolution is better than 2 cm^{-1} , and the spectra acquisition consisted of five accumulations of 60 s.

The high-resolution solid state ^{13}C NMR spectra were obtained at room temperature on a Bruker MSL 400 spectrometer at a frequency of 100.63 MHz for ^{13}C . The standard CPMAS pulse sequence was applied with a $6.5\text{ }\mu\text{s}$ ^1H - 90° pulse width, 3 ms contact pulses and 5 s repetition time. In the case of BaCO_3 a single pulse sequence was applied with $6\text{ }\mu\text{s}$ 90° pulses and 30 s repetition time. The spinning frequencies were, in all cases, of 4 KHz. The number of scans varied between 800 and 1600. All chemical shifts (δ) are given with respect to the TMS signal.

3. Experimental results

3.1. Powder precursor characterization

Fig. 1 shows the XRD pattern of the PR precursor, in which the amorphous character of the powders is preserved at this temperature. The FT-IR spectrum of the powder precursors is shown in Fig. 2. Although the IR spectrum of the PR powders was very complex but the presence of broad bands at 3445 cm^{-1} (water stretching vibrations),^{15,16} 2961 cm^{-1} (C–H stretching modes),¹⁷ 1736 cm^{-1} (C=O stretching modes for the ester group), 1625 and 1569 cm^{-1} (antisymmetric COO^- stretching mode for a unidentate complex and a bridging complex, respectively),¹⁸ 1389 cm^{-1} (stretching vibrations of a unidentate complex),¹⁹ the broad bands at 1450 , 1043 , 860 , and 622 cm^{-1} (assigned to carbonate ions)⁸ and, finally, broad bands at 776 and 545 cm^{-1} (Ti–O stretching modes), all of them characterized a relatively well dehydrated PR precursor.

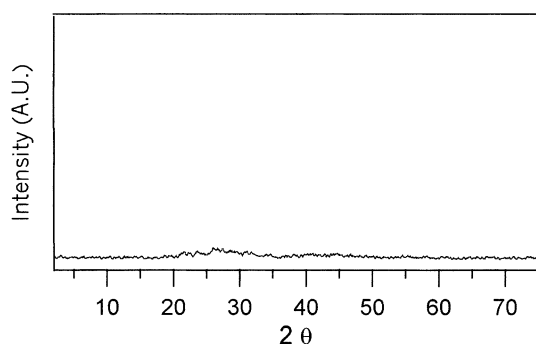


Fig. 1. XRD pattern of PR precursor powder.

The solid-state ^{13}C NMR spectrum of PR powder precursor is shown in Fig. 3. As it can be seen, the ^{13}C resonance absorption for the carboxyl groups, terminal- COOH at about 174 and 187 ppm, and middle- COOH at about 178 and 190 ppm, respectively, were present. A strong resonance signal at about 131.7 ppm can be representative of unsaturated carbon ($\text{C}=\text{C}$) produced in the dehydration of the PR powder. The two resonance signals at about 72 and 89.5 ppm attributable to the middle carbon, $\text{C}(\text{OH})$, were also observed. The presence of other functional groups as $-\text{CH}_2-$, which were not involved in the complexation process, was detected mainly by the resonance signal at 43 ppm.²⁰

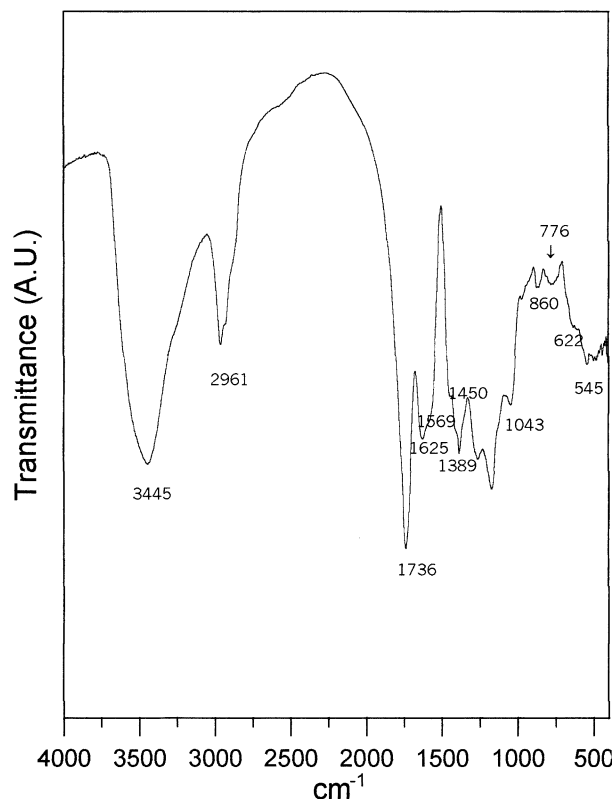


Fig. 2. FT-IR spectrum of PR powder.

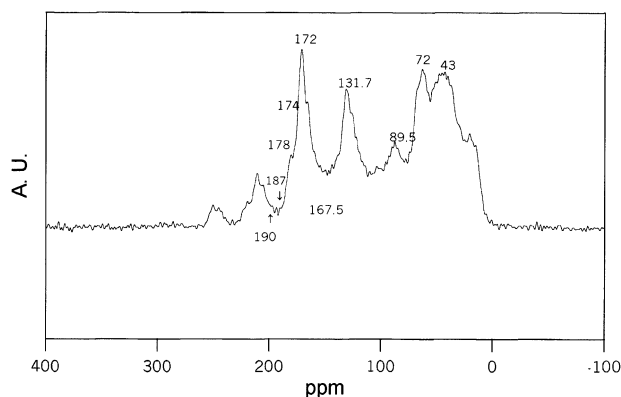


Fig. 3. Solid-state ^{13}C NMR spectrum of PR powder.

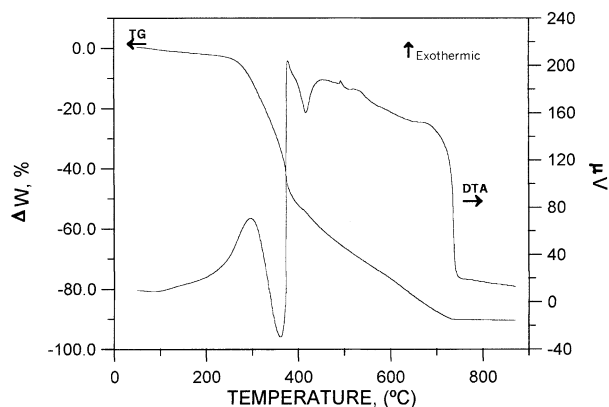


Fig. 4. TG and DTA curves of PR powder.

3.2. Thermal decomposition behavior of the powder precursors and characterization

Fig. 4 shows the TG/DTA curves at a heating rate of 10 °C/min in flowing air for PR powders between room temperature and 900 °C. The thermal decomposition of the PR precursor exhibited a multi-step exothermal process which is completed at about 740 °C. According to the TG curve, the thermal decomposition process is characterized by three apparent falls in sample weight over the temperature ranges from 200 to 360, 370 to 430, and 430 to 730 °C, respectively. Each of the falls in the TG curve corresponds to an exothermic peak in the DTA one. No endothermic effects were detected in the DTA curve. As previously reported elsewhere,¹⁰ given that no weight gain was registered through the thermal decomposition of PR precursor, we have to assume also now that the main reactions to be occurring with increasing temperature in the formation of BaTiO₃ from (Ba,Ti)-citrate polyester resin precursors, are the following: (a) dehydration of the PR precursors, (b) decomposition/oxidation of the dehydrated PR precursor with the formation of the intermediate phases, and (c) formation of barium titanate as a consequence of the reaction between the previously formed intermediate by-products.

Fig. 5 shows the FTIR spectra for the PR precursor calcined at different temperatures. The IR spectra of the PR amorphous powder showed bands at 3435, 2960, and 1760 cm⁻¹ corresponding to the O–H, C–H and C=O stretching modes, respectively. The sharp peaks at 1625 and 1569 cm⁻¹ are related to the antisymmetric COO⁻ stretching mode of unidentate complex and bridging complex, respectively. When calcined at 500 °C for 2 h, the peaks corresponding to the CO₃²⁻ group at about 1429, 1059, 856, and 693 cm⁻¹, and those corresponding to the carboxylate ions at 1558 and 1410 cm⁻¹ decreased in intensity. A broad band at about 574 cm⁻¹, which is typical of the Ti–O vibrations in the BaTiO₃ compound, starts to be developed. At this calcination temperature there are two extra peaks at about 874 and

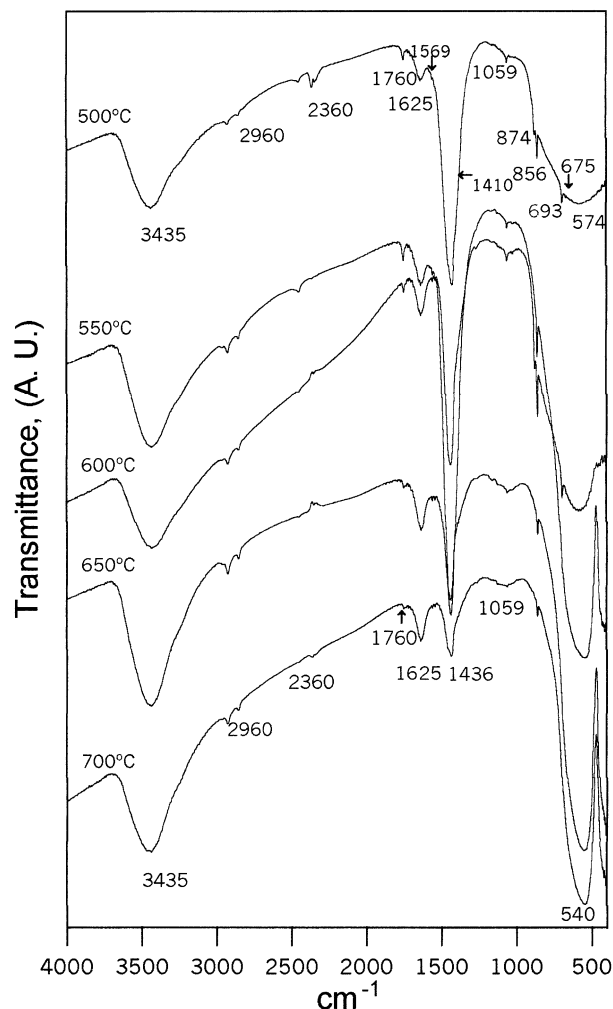


Fig. 5. FT-IR spectra of PR powders heat-treated at the indicated temperatures.

675 cm⁻¹, which could not be assigned to any bands of the barium oxide-titanium oxide system and they had been reported only by Gablenz et al.¹¹ A similar IR spectrum was observed when the PR precursor was calcined at 550 °C, although the peak at 674 cm⁻¹ disappeared and that at 874 cm⁻¹ decreased in intensity. Although it is not shown here, the peaks at 1435, 1059, 858, and 693 cm⁻¹, which are representative of the CO₃²⁻ group, were always quite broader than those assigned for the same CO₃²⁻ group in the BaCO₃ calcined at the same thermal conditions. These new IR structural features coincided, as we will see afterwards, with the fact that at this temperature interval, i.e. between 500 and 550 °C, the major phase detected by XRD was the oxy-carbonate intermediate one. With increasing calcination temperature above 550 °C, the mentioned extra IR peaks disappeared and the other IR bands decreased in intensity and almost disappeared at 700 °C. Simultaneously, the band corresponding to the Ti–O vibrations in BaTiO₃ was better developed and evolved up to a constant frequency value of 543 cm⁻¹.

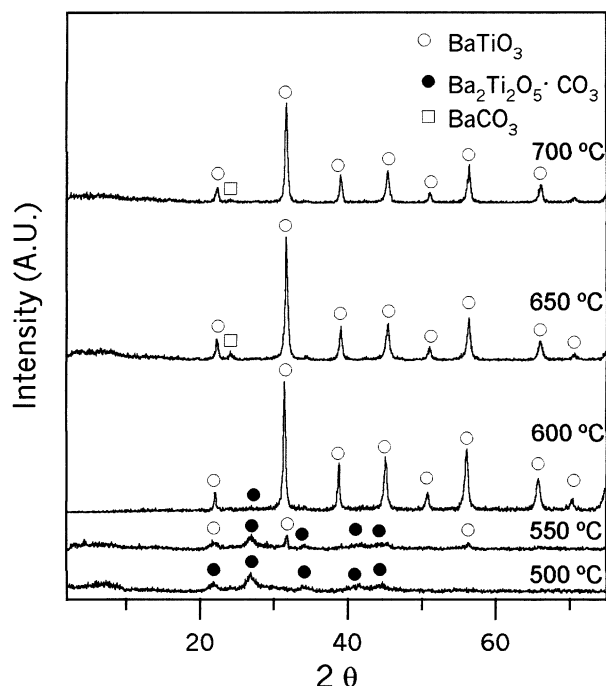


Fig. 6. XRD patterns showing the phases evolution with calcination temperature of PR powders.

The phase development with increasing calcination temperature in the PR powders, was also studied by XRD and Raman spectroscopy on the calcined samples in the temperature range of 500–750 °C at a heating rate of 10 °C/min. Fig. 6 shows the XRD patterns for PR calcined powders. As previously shown, the PR powder fired at 250 °C was amorphous in structure, and such a broad continuum in the XRD patterns was also present after calcining up to 400 °C for 2 h. Above that temperature and up to 550 °C only broad diffraction reflections, which could be clearly identified as to correspond mainly to the so-called intermediate oxycarbonate phase, ($\text{Ba}_2\text{Ti}_2\text{O}_5\text{CO}_3$), claimed by Kumar et al.⁹ and corroborated by Arima et al.²¹ were present, although some of these diffraction peaks can also be attributable to a residual BaCO_3 , to an oxygen-deficient TiO_{2-x} or to an incipient hexagonal BaTiO_3 . Above 550 °C the BaTiO_3 began to be formed and the oxycarbonate phase slowly decreased and almost disappeared at about 600 °C. Simultaneously to the disappearance of the oxycarbonate intermediate phase, BaCO_3 was formed and also disappeared above 700 °C. These results are discrepant with the previous contention of Hennings and Mayr⁸ and Vasylykiv et al.,¹² whose precluded and even questioned the existence of the so-called oxycarbonate intermediate phase ($\text{Ba}_2\text{Ti}_2\text{O}_5\text{CO}_3$).

At this point, it should be noted that between 600 and 750 °C a broad peak at about 45.2° was always present in our XRD data and no clear splitting could be detected. XRD patterns for powders heat-treated within that temperature interval were indexed on a m3m cubic unit

cell and a lattice parameter of $a = 0.4041 \pm 0.0005$ nm was measured, which is in close agreement with that of Busca et al.¹⁷ ($a = 0.4036$ nm). The particle size of the powders shifted from 15 nm at 600 °C to 30 nm at 750 °C. At this temperature interval there are serious line broadening effects due to the small size of the formed BaTiO_3 particles, and for this reason it becomes difficult to distinguish between cubic and tetragonal barium titanate phases by means of XRD techniques. Above 900 °C the XRD reflections became sharper and a gradual splitting of the pseudocubic [200] into tetragonal [200] and [002] was observed. Then the XRD patterns of the powders were indexed on a 4mm tetragonal unit cell. Lattice parameters were measured and a c/a ratio value close to 1.01 could be calculated, for samples in which a clear splitting was apparent (≥ 1100 °C, (see Fig. 7).

In order to support the above statements the PR powder calcined in the 500–700 °C temperature range was characterized using room temperature Raman spectroscopy. Fig. 8 shows the Raman spectra for PR calcined powders. The Raman spectrum of the PR powder calcined at 500 °C exhibited a fluorescent-like background and only a broad band at 832 cm^{-1} and a sharper band at 1064 cm^{-1} were detected. This last Raman band could be assigned to the CO_3^{2-} symmetric stretching mode. The spectrum of the PR precursor calcined at 600 °C for 2 h showed some new relevant features: (i) the intensity of the peak representing the CO_3^{2-} ions strongly decreased, (ii) the peak frequency shifted up to a value of 1059 cm^{-1} , (iii) the appearance of new broad bands at 721, 517, 305 and 260 cm^{-1} which are characteristics of the BaTiO_3 with tetragonal structure, and (iv) another new band at about 638 cm^{-1} started to be developed, which can be attributed to an incipient BaTiO_3 with hexagonal structure.²³ With increasing calcination temperature, both the Raman bands for tetragonal and hexagonal BaTiO_3 polymorphs increased in intensity up to 650 °C, and the band representative of the CO_3^{2-} group almost disappeared. The shift of the carbonate ions peak frequency from about 1064 to 1059 cm^{-1} above 550°, can be related with the formation of some amount of BaCO_3 following the hypothetical decomposition of the oxycarbonate intermediate phase, which rapidly reacts with residual titanium oxide. The disappearance of the main carbonate ion peak supported the above contention.²⁴

It must be noted here that since the Raman spectroscopy is much more sensitive to prove the local rather than long ranges structure, the presence of a peak at about 305 cm^{-1} in the spectrum of the sample heat-treated at 600 °C indicates, at least on a local scale, asymmetry within the TiO_6 octahedra of the BaTiO_3 structure and, contrarily to the XRD results, the as prepared powders are tetragonal rather than cubic. It could be suggested that the symmetry of the crystals as

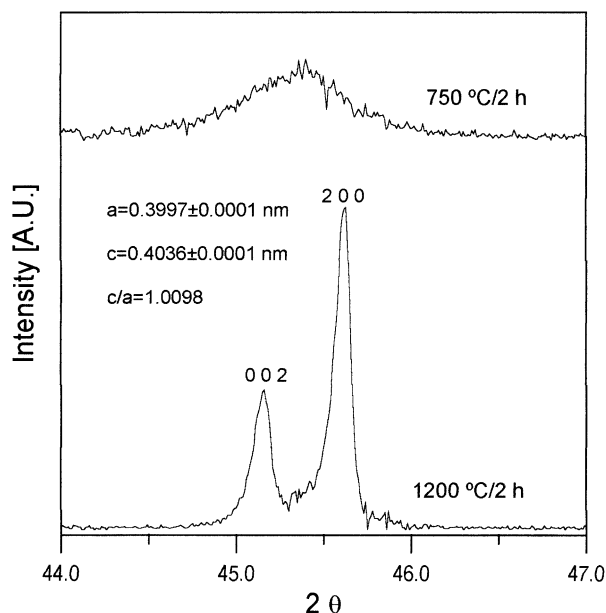


Fig. 7. XRD diffractograms over the 2θ range $44\text{--}47^\circ$ of BaTiO_3 after calcining at the indicated temperatures.

observed by Raman spectroscopy indicates a local and dynamic symmetry, and the symmetry determined by XRD measurements is an average and static symmetry.

3.3. Synthesis, structural features and thermal stability of the intermediate oxycarbonate phase

In order to establish as unambiguously as possible the existence of the “so-called” intermediate oxycarbonate $\text{Ba}_2\text{Ti}_2\text{O}_5\cdot\text{CO}_3$ phase prior to the BaTiO_3 formation, the PR powder was milled for 2 h and sieved below $100\text{ }\mu\text{m}$. Such a fine PR powder was calcined at a heating rate of $10^\circ\text{C}/\text{min}$ at $500\text{--}550^\circ\text{C}$ for 2 h. To know its thermal behavior, the synthesized oxycarbonate phase was studied by differential thermal analysis and its stability was studied by XRD on the isothermally heat-treated samples at the $480\text{--}524^\circ\text{C}$ temperature interval for several hours.

Fig. 9 shows the XRD pattern of the synthesized oxycarbonate phase in air from the PR precursor and as it is clearly shown, a poorly crystallized phase but well different to both BaCO_3 or BaTiO_3 was developed. Even more, no diffraction peaks corresponding to these last two phases were detected. Therefore, although not well crystallized, we are in the presence of a new phase whose main diffraction peaks were detected at $2\theta = 21.8^\circ$ (56), 24.2° (37), 26.8° (100), 30.2° (32), 32.3° (29), 33.8° (41), 40.8° (40), 44.9° (47), and 54.4° (10) (in parentheses the relative peak intensity). These diffraction peaks closely coincide with those found for the intermediate oxycarbonate phase claimed by Kumar et al.⁹ and Arima et al.²¹

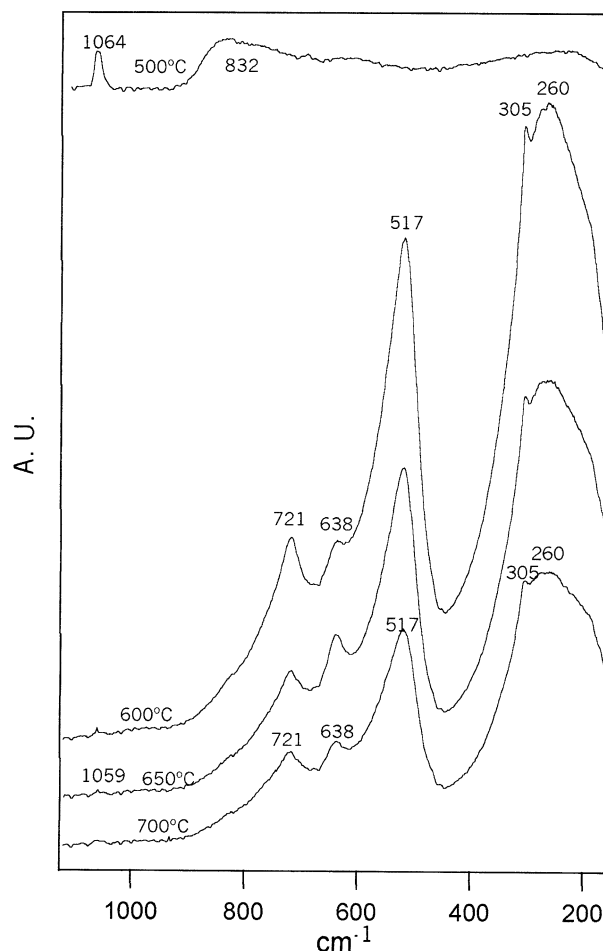


Fig. 8. Raman spectra of PR powder after heat-treatment at the indicated temperatures.

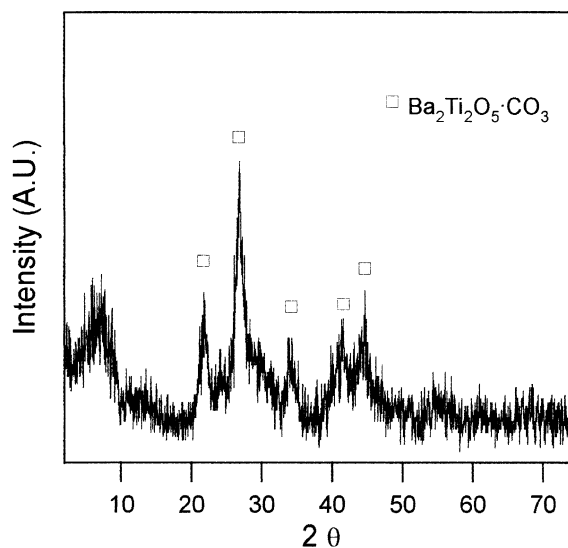


Fig. 9. XRD pattern of PR powder after calcining at 500°C for 2 h showing the predominance of the oxycarbonate intermediate phase without any barium carbonate.

The TG/DTA curves, as shown in Fig. 10, recorded on the synthesized oxycarbonate intermediate phase shows a wide exothermal effect between room temperature and about 690 °C, which can be attributed to the decomposition–oxidation of the residual organics, and a relatively small endothermic peak between 690 and about 750 °C which can be attributed to the thermal decomposition of the oxycarbonate intermediate phase. The weight loss between room temperature and about 690 °C was near 3%, and between 690 and 800 °C was about 6.2% which is slightly lower than that measured by Kumar et al.⁹ for the thermal decomposition of this oxycarbonate phase (8.1%).

Fig. 11 shows comparatively the IR spectra recorded for the synthesized oxycarbonate phase at 500 and

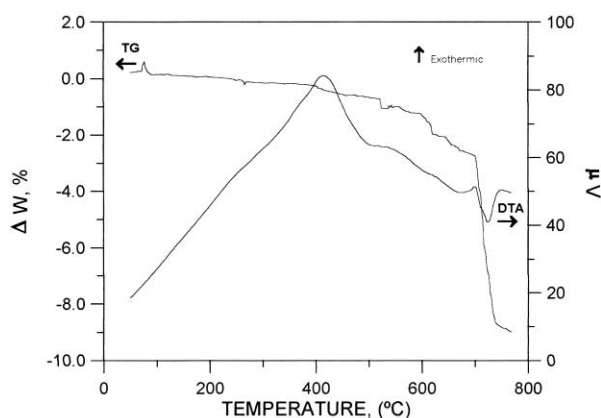


Fig. 10. TG and DTA curves for the oxycarbonate intermediate phase.

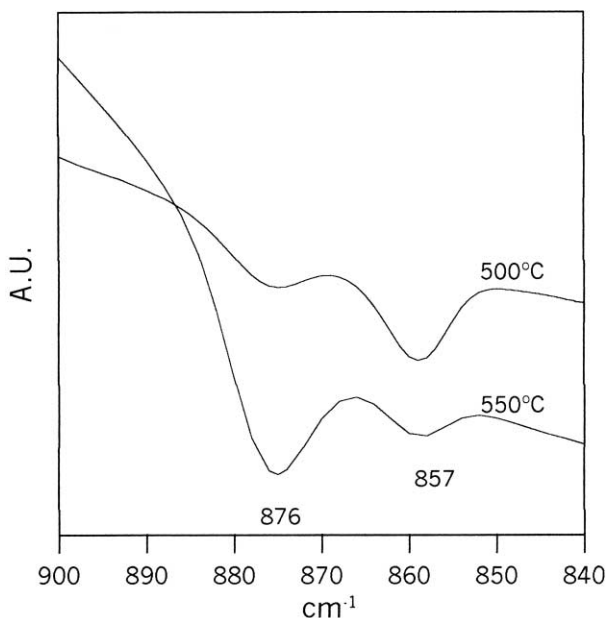


Fig. 11. FT-IR spectra of PR powder heat-treated at 500 and 550 °C for 2 h showing the appearance of new IR features for the synthesized oxycarbonate intermediate phase.

550 °C. Two significant features are to exist: (i) the appearance of a new peak at 876 cm^{-1} which can not be assigned to any of the barium oxide-titanium oxide system,¹¹ along with the almost disappearance of the typical IR peak of the pure orthorhombic barium carbonate, and (ii) the IR bands at 1430, 1060, 858, and 692 cm^{-1} as representatives of the CO_3^{2-} group, not shown here, are much broader for this oxycarbonate intermediate phase.

When comparing the Raman spectrum of this intermediate phase with that of the BaCO_3 powder (see Fig. 12), a significant difference in the frequency of the characteristic peak for CO_3^{2-} ions at about 1066 cm^{-1} , which is quite higher and broader than that for pure BaCO_3 (1058 cm^{-1}), was also found.

Fig. 13 shows the solid-state ^{13}C NMR spectrum of the synthesized oxycarbonate intermediate phase, $\text{Ba}_2\text{Ti}_2\text{O}_5\text{CO}_3$. For comparison, the ^{13}C NMR spectrum of pure BaCO_3 is also shown. Several broad resonance signals appeared mainly those at 51, 87.8, 128.5, 168.8, and 209.3 ppm which can not be assigned to BaCO_3 and, if any, as it would be the case for the resonance absorption at 168.8 and 209.3 ppm, the signals were much broader and with chemical shift smaller than

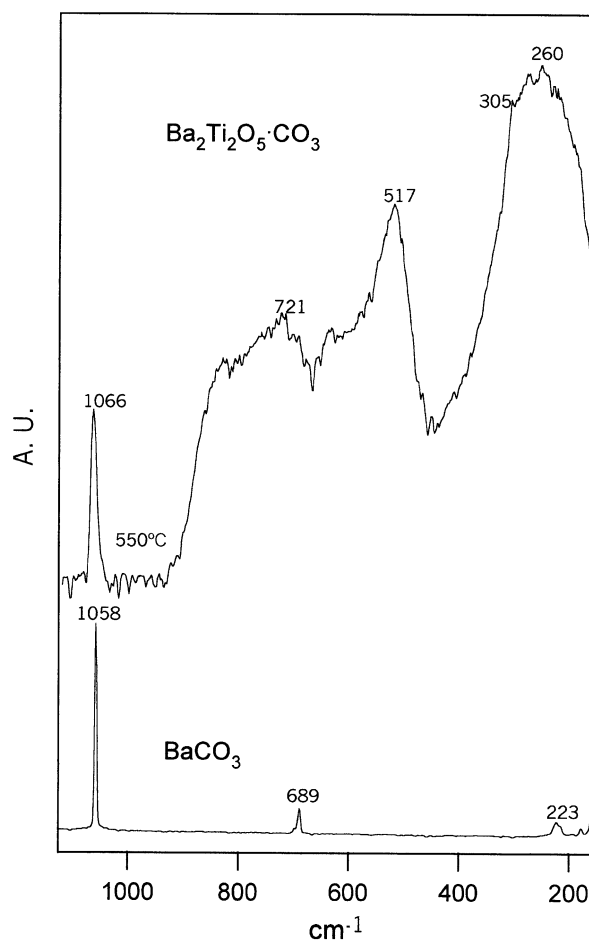


Fig. 12. Raman spectra for barium carbonate and oxycarbonate intermediate phase.

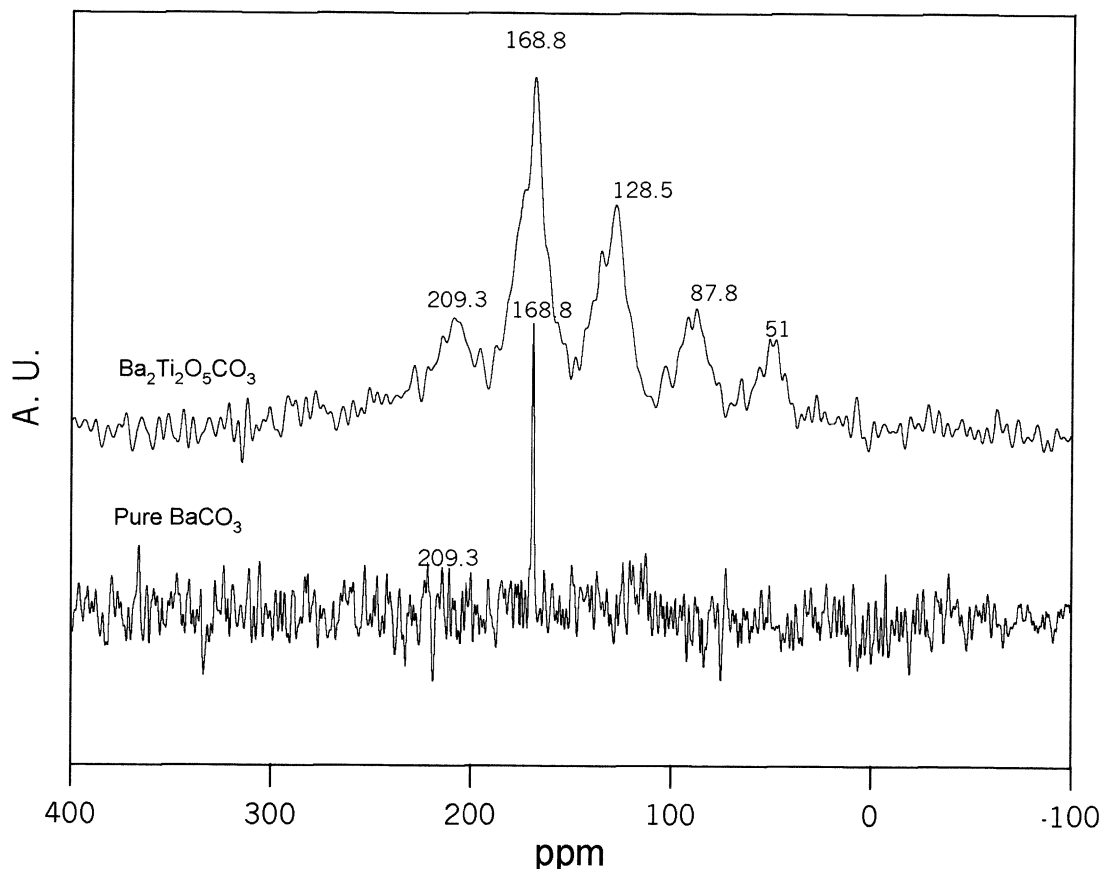


Fig. 13. ^{13}C NMR spectra for the synthesized oxycarbonate intermediate phase ($\text{Ba}_2\text{Ti}_2\text{O}_5\text{CO}_3$) and pure BaCO_3 .

those of BaCO_3 . Therefore, even assuming comparable positions for those resonance peaks hypothetically attributable to BaCO_3 , but their broadening and the absence of that compound as suggested by the XRD measurement (see Fig. 9), the new ^{13}C NMR resonance signals have to be assigned to the carbonate ions of the intermediate phase $\text{Ba}_2\text{Ti}_2\text{O}_5\text{CO}_3$ in close agreement, on the other side, with the Rajendran and Suba Rao²⁵ and Tsay et al.²² results.

Fig. 14a–f shows the XRD evolution of the synthesized oxycarbonate intermediate with increasing temperature. As it can be observed, the amount of the oxycarbonate phase first slightly increased with both the temperature and the heat-treatment time up to 495 °C (see Fig. 14c), and as soon as the BaTiO_3 began to be formed the amount of the oxycarbonate phase slowly decreased and almost disappeared after a heat-treatment for 20 h at 524 °C. From these results it seems clear that the oxycarbonate phase is stable within a relatively wide temperature range, and its transformation is the rate-controlling step for the BaTiO_3 formation. Given that the heating rate used for the synthesis of the oxycarbonate phase was relatively high (10 °C min^{-1}), it can be suggested that such a phase was formed as consequence of a transitory frozen non-equi-

librium state in the beginning of an initial reaction between nanosized BaCO_3 and amorphous TiO_2 , prior to the formation of the nanosized tetragonal and hexagonal BaTiO_3 polymorphs as the final products. Based on the whole of the above results we can propose a possible coordinated structure of the oxycarbonate phase as illustrated in Fig. 15. The same takes into account the suggestions of Gablenz et al.¹¹ and Tsay et al.¹⁵

4. Discussion

The study of the thermal decomposition behavior of (Ba,Ti)–metal citrate polymerized resin in previous reports, was carried out by directly heating the polymerized resin at a predetermined heating rate in air.^{8,9,21} Hennings and Mayr⁸ and Arima et al.²¹ assumed a molecular-level mixing of cations in the solution precursor, and that basically the coordination of barium and titanium cations did not change on polymerization even in the pyrolysed resin at a temperature below 400 °C. On such a basis, the attained results on the reaction mechanism for the BaTiO_3 formation were very far of being coincident. A solid-state reaction between

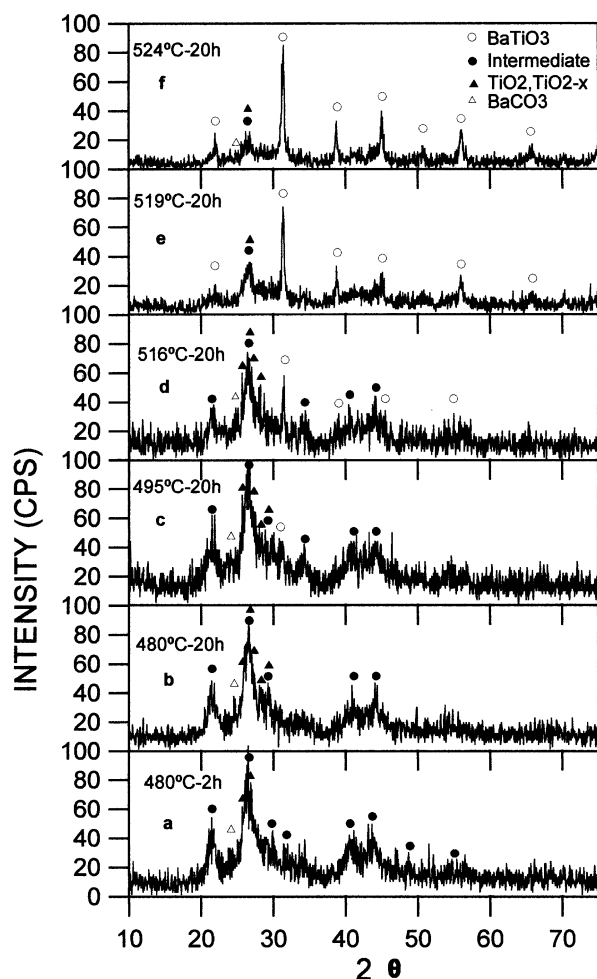


Fig. 14. Stability of the oxycarbonate intermediate phase with increasing temperature.

nanosized BaCO_3 and amorphous TiO_2 in the first of them,⁸ and the formation of an oxycarbonate $\text{Ba}_2\text{Ti}_2\text{O}_5\cdot\text{CO}_3$ intermediate in the other two,^{9,21} were their conclusions. More recently, Tsay et al.^{15,22} reported the formation of a metastable oxycarbonate intermediate phase with the structure of BaTiO_3 with carbonate ions located within the BaTiO_3 interlayer. On the other hand, no influence of the pH of the (Ba,Ti)–metal citrate solution precursor on the BaTiO_3 formation mechanism was also suggested, albeit the structure of the synthesized BaTiO_3 was not established.

Although the development of intermediate phases during the thermal decomposition of (Ba,Ti)–citrate polymerized precursors has been controversially disputed in the last 10 years, but no clear distinguishable structure features for the so-called oxycarbonate intermediate phase, $\text{Ba}_2\text{Ti}_2\text{O}_5\cdot\text{CO}_3$, were reported. However, it is commonly accepted that such an intermediate phase is the key compound in the BaTiO_3 formation mechanism when polymerized organic precursors are used.²⁶

From Fig. 6, it can be clearly seen that the direct heating of (Ba,Ti)–citrate polyester resin led to the

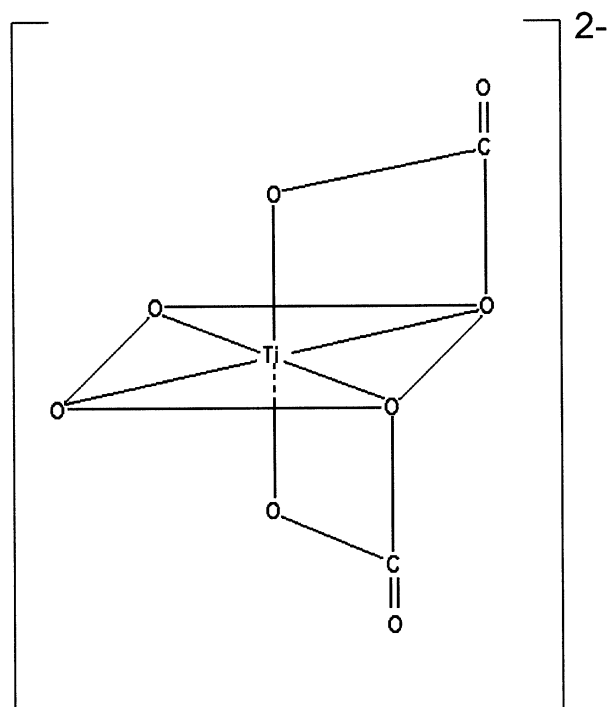


Fig. 15. Tentative structure for the oxycarbonate phase.

BaTiO_3 formation via an oxycarbonate, $\text{Ba}_2\text{Ti}_2\text{O}_5\text{CO}_3$ intermediate phase. Tsay et al.¹⁵ claimed, for the first time, that the oxycarbonate intermediate had been unambiguously established taken into account their XRD and IR experimental results. Some broadening in the IR bands at 1425, 1050, and 860 cm^{-1} related to the carbonate ions with respect to those of the pure BaCO_3 , and the appearance of some broad peaks in the XRD data of samples calcined at 500 and 550 $^\circ\text{C}$ allowed them to support the above statement. From our IR, XRD, Raman, and ^{13}C NMR data (see Figs. 5–13), new structural features are contributing to a better knowledge of such intermediate phase. For example, our oxycarbonate intermediate phase is better characterized not only by the XRD data showing a not well crystallized single-phase (without the presence of any residual BaCO_3) (see Fig. 9), but also by the appearance of an extra peak at 875 cm^{-1} in the IR spectrum of those PR samples calcined at 500 and 550 $^\circ\text{C}$ for 2 h, along with the already mentioned broadening of the IR bands related to the carbonate ions in the samples, see Fig. 11. It means a displacement of the frequency for this specific vibration mode as high as 18 cm^{-1} with respect to the typical of pure BaCO_3 (857 cm^{-1}). Such a frequency, which is typical of calcite (CaCO_3), is indicating a different crystallographic environment for the carbonate ions in the oxycarbonate intermediate phase and, as suggested by Gablenz et al.,¹¹ and Tsay et al.,¹⁵ the carbonate ions can be considered as components of the nanosized oxycarbonate phase structure. Besides this, our Raman experimental results (see Fig. 12), show

new features which characterized the oxycarbonate intermediate phase. The shift of the peak related to the carbonate ions from 1058 cm^{-1} (typical for pure BaCO_3) towards higher frequencies, 1064 cm^{-1} in PR samples heat-treated at 500°C , and to 1066 cm^{-1} in those PR samples heat-treated at 550°C for 2 h (see Figs. 8 and 12), along with a strong increasing in intensity of the carbonate ions peak, confirm this as a differential characteristic of such an oxycarbonate intermediate phase developed when the starting raw materials used for the BaTiO_3 synthesis is a (Ba, Ti)-polyester resin. A similar phenomenon was also founded by Arima et al.²¹ but it was not supported by other experiments. The presence in the Raman spectrum of the sample calcined at 550°C of broad bands related to an incipient BaTiO_3 can be supporting, on the other side, the suggestion of a BaTiO_3 with interlayered CO_3^{2-} groups as the structure for the oxycarbonate $\text{Ba}_2\text{Ti}_2\text{O}_5\cdot\text{CO}_3$ intermediate phase.²² Finally, the much broader resonance signals for the carbonate ions in the ^{13}C NMR spectrum for such an oxycarbonate phase (see Fig. 13), supported the above contention. The whole of all these results allowed us to assume a particular bonding state of the carbonate ions for the synthesized oxycarbonate phase, along with a certain electronic interaction between carbon and titanium,¹¹ such as it is proposed in a tentative form in Fig. 15.

Above 550°C , the XRD patterns showed considerable peak broadening associated with the nanosized particle size and, therefore, poor crystallinity of the BaTiO_3 powders. According to our results (see Fig. 7), no evidence for splitting appeared which can lead to assume a pseudo-cubic structure for the formed BaTiO_3 at this thermal level as reported elsewhere.²⁷ However, as it was previously suggested,¹⁰ the appearance of a peak at about 305 cm^{-1} in the Raman spectra is indicating a certain distortion of Ti–O bonds within the TiO_6 octahedra of BaTiO_3 . This fact allowed us to assume that the nanosized BaTiO_3 powders do not have cubic symmetry. On the other hand, the presence of a Raman band at about 638 cm^{-1} which increased in intensity with the calcination temperature (see Fig. 8), could be attributed to TiO_2 but the absence of its main Raman peak at 141 cm^{-1} precluded such an assignment. Therefore, the Raman band at 638 cm^{-1} can be considered as representative of the strongest scattering from the BaTiO_3 with hexagonal structure,²³ which can be stabilized at low-temperature by the high surface free energy of the nanosized BaTiO_3 powders. From this whole of results it can be advanced that the nanosized powders prepared by thermal decomposition of a (Ba,Ti)-citrate polymeric organic complex in air, consisted of a mixture of the tetragonal and hexagonal BaTiO_3 polymorphs rather than cubic. Such a contention can be contradictory to the widely accepted critical particle size theory for the stabilization of the cubic BaTiO_3 polymorph,^{27–29} but it is in close agreement

with similar results attained on submicronised BaTiO_3 powders prepared by the hydrothermal and sol-gel synthesis methods.^{30,31} In summary, it could be suggested that the structure of the BaTiO_3 powders calcined in the $550\text{--}750^\circ\text{C}$ temperature range has a tetragonal 4mm symmetry at the local level, and a cubic m3m symmetry as the average one. This suggestion implies the assumption of some disordering in the crystal structure of the nanosized BaTiO_3 powders.

5. Conclusions

The thermal decomposition in air of (Ba, Ti)-citrate complex precursors has proven to be an efficient route for the preparation of nanosized agglomerated powders of stoichiometric BaTiO_3 . It has been established that previous heat-treatments of such a complex precursor at 250° led to a polyesterified amorphous resin. Starting from this raw materials we can advance the following suggestions: (1) the BaTiO_3 synthesis takes place via the formation of an oxycarbonate phase, $\text{Ba}_2\text{Ti}_2\text{O}_5\cdot\text{CO}_3$, as the main intermediate, (2) although not well crystallized, the oxycarbonate intermediate phase has been synthesized at the temperature interval of $500\text{--}550^\circ\text{C}$. The weight loss measured from the TG curve, the XRD data, and the new IR and Raman structural features have been identified as distinguishable characteristics for such an oxycarbonate phase. Along with the unique XRD pattern, the appearance of a new IR band for the out-of-plan vibrations modes of the carbonate ions, the clear shift in the wave numbers of the carbonate ions in the Raman spectra, and the broadening phenomenon of the ^{13}C NMR resonance signals, enable us to suggest that such an oxycarbonate phase has a formula close to $\text{Ba}_2\text{Ti}_2\text{O}_5\cdot\text{CO}_3$, in whose proposed structure the carbonate ions are different to those of pure BaCO_3 , being probably located within the BaTiO_3 interlayers,²² (3) Based on the XRD data, Raman spectra, and crystal size measurements, the BaTiO_3 powders as synthesized in the temperature range of $550\text{--}750^\circ\text{C}$ consisted of a mixture of tetragonal and hexagonal phases rather than cubic. Raman spectra of BaTiO_3 powders with a particle size as small as $15\text{--}20\text{ nm}$ showed evidence for asymmetry within the TiO_6 octahedra of the BaTiO_3 lattice. On the other hand, the presence of the high-temperature hexagonal BaTiO_3 polymorph at low-temperature can be justified by the extremely high surface free energy of the nanosized particles that can stabilized such a phase.

Acknowledgements

This work has been supported by the Spanish CICYT Grant No. MAT 97-0694-C 02-01.

References

- Clabaugh, W. S., Swiggard, E. M. and Gilchrist, R., Preparation of barium titanyl oxalate tetrahydrate for conversion to barium titanate of high purity. *J. Res. Natl. Bur. Stand.*, 1956, **56**, 289–291.
- Gallagher, P. K. and Thomson, J. Jr., Thermal analysis of some barium and strontium titanyl oxalates. *J. Am. Ceram. Soc.*, 1965, **48**, 644–647.
- Pechini, M. P., Method of preparing lead and alkaline earth titanates and niobates and coating method using the same for a capacitor. US Patent No. 3330697, 11 July 1967.
- Mulder, B. J., Preparation of BaTiO₃ and other ceramic powders by coprecipitation of citrates in alcohol. *Am. Ceram. Soc. Bull.*, 1970, **40**, 90–93.
- Lessing, P. A., Mixed-cation oxide powders via polymeric precursor. *Am. Ceram. Soc. Bull.*, 1989, **68**, 1002–1007.
- Cho, S. G., Johnson, P. F. and Condrate, R. A., Thermal decomposition of (Sr,Ti) organic precursors during the Pechini process. *J. Mater. Sci.*, 1990, **25**, 4738–4744.
- Gopalakrishnamurthy, H. S., Rao, M. S. and Kutty, T. R. N., Thermal decomposition of titanyl oxalates—I. Barium titanyl oxalate. *J. Inorg. Nucl. Chem.*, 1975, **37**, 891–898.
- Hennings, D. and Mayr, W., Thermal decomposition of (Ba,Ti) citrates into barium titanate. *J. Solid State Chem.*, 1978, **26**, 329–338.
- Kumar, S., Messing, G. L. and White, W. B., Metal organic resin derived barium titanate: I, formation of barium titanium oxycarbonate intermediate. *J. Am. Ceram. Soc.*, 1993, **76**, 617–624.
- Durán, P., Capel, F., Tartaj, J. and Moure, C., BaTiO₃ formation by thermal decomposition of a (Ba,Ti)-citrate polyester resin in air. *J. Mater. Res.*, 2001, **16**, 197–209.
- Gablenz, S., Abicht, H. P., Pippel, E., Lichtenberger, O. and Wotersdorf, J., New evidence for an oxycarbonate phase as an intermediate step in BaTiO₃. *J. Eur. Ceram. Soc.*, 2000, **20**, 1053–1060.
- Vasyl'kiv, O. O., Ragulya, A. V. and Skorodhod, V. V., Theory and technology of sintering, heat and chemical heat treatment. *Powder Metallurgy and Metal Ceramics*, 1997, **36**, 277–282.
- Cho, W. S., Structural evolution and characterisation of BaTiO₃ nanoparticles synthesised from polymeric precursors. *J. Phys. Chem. Solids*, 1998, **59**, 659.
- Cullity, B. D., *Elements of X-ray Diffraction*, 2nd edn. Addison-Wesley, Reading, MA, 1978 pp. 360–363.
- Tsay, J. D., Fang, T. T., Gubiotti, T. A. and Jying, Y., Evolution of the formation of barium titanate in the citrate process: the effect of the pH and the molar ratio of barium ion and citric acid. *J. Mater. Sci.*, 1998, **33**, 3721–3727.
- Coutures, J. P., Odier, P. and Proust, C., Barium titanate formation by organic resin formed with mixed citrates. *J. Mater. Sci.*, 1992, **27**, 1849–1856.
- Busca, G., Buscaglia, V., Leoni, M. and Nanni, P., Solid state and surface spectroscopy characterisation of BaTiO₃ powders. *Chem. Mater.*, 1994, **6**, 955–961.
- Nakamoto, K., *Infrared and Raman Spectra of Inorganic and Coordination Compounds*, 4th edn. Wiley Press, New York, 1986 p. 231.
- Stokenhuber, M., Mayer, H. and Lercher, J. A., Preparation of barium titanate from oxalates. *J. Am. Ceram. Soc.*, 1993, **76**, 1185–1190.
- Breitman, E. and Voelter, W., *¹³C-NMR Spectroscopy*. Verlag Chemie, New York, 1978.
- Arima, M., Kakihana, M., Nakamura, Y., Yasima, M. and Yoshimura, M., Polymerised complex route to barium titanate powder using barium-titanium mixed-metal, citric acid complex. *J. Am. Ceram. Soc.*, 1996, **79**, 2847–2856.
- Tsay, J. D. and Fang, T. T., Effects of molar ratio of citric acid to actions and of pH value on the formation and thermal decomposition behaviour of barium titanium citrate. *J. Am. Ceram. Soc.*, 1999, **82**, 1409–1415.
- Erör, N. G., Lohrer, T. M. and Cornilsen, B. C., Low-temperature hexagonal BaTiO₃ polymorph and carbonate adsorption. *Ferroelectrics*, 1980, **28**, 321–324.
- Wang, J., Fang, J., Ng, S. C., Gan, L. M., Chew, C. H., Wang, X. and Shen, Z., Ultrafine barium titanate powders via microemulsion processing routes. *J. Am. Ceram. Soc.*, 1999, **82**, 873–881.
- Rajendran, M. and Rao, M. S., Formation of BaTiO₃ from citrate precursor. *J. Solid State Chem.*, 1994, **113**, 239–247.
- Hennings, D., Rosenstein, G. and Schreinemacher, H., Hydrothermal preparation of barium titanate from barium-titanium acetate gel precursors. *J. Eur. Ceram. Soc.*, 1991, **8**, 107–115.
- Uchino, K., Sadanaga, E. and Irose, T., Dependence of the crystal structure on particle size in barium titanate. *J. Am. Ceram. Soc.*, 1989, **72**, 1555–1558.
- Hennings, D. and Schreinemacher, H., Characterisation of hydrothermal barium titanate. *J. Eur. Ceram. Soc.*, 1992, **9**, 41–46.
- Begg, B. D., Vance, E. R. and Novotny, J., Effect of the particle size on the room-temperature crystal structure of barium titanate. *J. Am. Ceram. Soc.*, 1994, **77**, 3186–3192.
- Frey, M. H. and Payne, D. A., Grain size effect on structure and phase transformation for barium titanate. *Physical Review B*, 1996, **54**, 3154–3168.
- Clark, I. J., Takeuchi, T., Ohtori, N. and Sinclair, D. C., Hydrothermal synthesis and characterisation of BaTiO₃ fine powders: precursors, polymorphism and properties. *J. Mater. Chem.*, 1999, **9**, 83–91.